

Superconductor-ferromagnet tunneling measurements indicate *sp*-spin and *d*-spin currents

M. Münzenberg* and J. S. Moodera

Francis Bitter Magnet Laboratory, Massachusetts Institute of Technology, Cambridge, Massachusetts 02139, USA

(Received 5 May 2004; published 10 August 2004)

Spin polarization of tunneling electrons was observed to decrease as the barrier thickness decreased. The polarization measured by the Meservey-Tedrow technique has been separated into a positively and a negatively spin polarized current arising from *sp*- and *d*-like interfacial states. The model for separating *sp*- and *d*-like spin currents is expressed with an interface transmission probability, a decay rate within the barrier and polarization for each of the channels. The present observation can also have an impact on the downscaling of TMR elements.

DOI: 10.1103/PhysRevB.70.060402

PACS number(s): 74.50.+r, 72.25.Mk, 73.40.Gk, 75.30.-m

Transition metal ferromagnets and alloys show only 50% or less¹⁻⁴ positive spin polarization in tunneling experiments resulting in a TMR signal of nearly 50%. The question arises as to what are the fundamental limits on the resistance and magnetoresistance of ferromagnetic to ferromagnetic (FM/I/FM) tunnel junctions. A way to increase the TMR signal is to search for materials with high *interfacial* spin polarization. On the other hand for the downscaling of TMR devices ultra transparent tunnel barriers are required which have not been systematically explored with accompanying impact on the spin polarization. In both cases controlled experiments and understanding of the spin-polarized transport through a tunnel barrier is still missing. Some progress has been made over the years towards understanding of the tunneling process from the theoretical⁵⁻¹² and experimental points of view.^{2,13-18} Here we present experiments and analysis to address the fundamental issues: the *sp*-like and *d*-like electronic contributions to the spin polarized current as measured by a spin split superconducting spin detector using planar tunnel junctions.

Soon after the discovery of spin splitting of quasiparticle states in superconductors (SC) (Ref. 1) it was used as a detector to determine the spin polarization of ferromagnets in a tunneling experiment. From the beginning, the sign of the spin polarization P was a subject of intense discussion and it is still debated. Stearns developed a two current model consisting of majority and minority spin currents flowing in parallel.⁵ Heavy *d*-electrons provide most of the magnetization of transition metals but are quite localized while itinerant electrons, dominating the spin transport, are polarized by exchange interaction with the localized *d*-electrons consequently having a smaller polarization with opposite sign. Based on this model understanding the origin of positive sign (majority spins) observed in spin polarized tunneling experiment is straightforward. In other words, a high spin polarization P is related to heavy *d*-like pockets in the Fermi surface with a low Fermi velocity (and hence low contribution to the tunnel current) while light *sp*-like electrons, highly mobile, dominate the spin currents. Mazin¹² has recently discussed the correct way to describe the polarization in a transport experiment—to define the spin polarization by the polarization of two currents $i_{j,\text{FM}}$ ($j=sp$ and d) leading to a polarization weighted by the Fermi velocity squared.

At the interface with the insulator, bonding can suppress or promote contributions to the tunneling current as it was clearly observed in some recent experiments.^{16,17} The currents with different symmetries j thus have to be weighted with a transfer function M_j for the interface (current at the interface, $i_{j,0}$). This is described by the matching of the Fermi surface of the majority and minority spins in the FM to the complex interface Fermi surface of the insulator,

$$i_{j,0} = M_j i_{j,\text{FM}}. \quad (1)$$

In addition, the interfacial currents at the insulator interface have a characteristic exponential decay length κ_j^{-1} for each band with symmetry j (Ref. 19) into the barrier (current within the barrier, i_j),

$$i_j = i_{j,0} e^{-\kappa_j t}. \quad (2)$$

Since the *d* states decay much faster within the barrier (of thickness t) than the *sp* states, as a consequence in the limit of a thick barrier $t \gg \kappa_d^{-1}$ only *sp*-like states will contribute to the tunneling current. In Fig. 1 the normalized current is plotted for $\kappa_d^{-1} = 0.5 \text{ \AA}$, $i_{d,0} = 0.9$ and $\kappa_{sp}^{-1} = 0.68 \text{ \AA}$, $i_{sp,0} = 0.1$. At 10 \AA the contribution from *d*-like states has dropped below 5%.

In a related experimental study the tunneling from a magnetic Ni scanning tunneling microscope (STM) tip into GaAs was measured by Alvarado.¹⁹ Surprisingly, in contrast to spin polarized tunneling in planar junctions, a negative polarization of the tunneling current was observed and ascribed to the *d* states, giving rise to new speculations on the tunneling models. The question arises if it is possible to observe the contribution of the *d* states in a planar spin polarized tunneling device if the barrier thickness is reduced below 10 \AA towards the limit of ultrathin tunneling barriers?

In the following experiments spin up and down currents in a superconducting Al/Al₂O₃/Fe tunnel structure are separated using the Zeeman splitting of the quasiparticle density of states in the superconducting Al film, the Meservey Tedrow technique.¹ The superconducting electrode Al is oxidized directly to form a tunnel barrier of any thickness with excellent control and quality. Therefore it has essentially the same properties for different oxidation times even in the limit of ultratransparent barriers. Careful oxidation has been carried out for various oxygen partial pressures ranging from

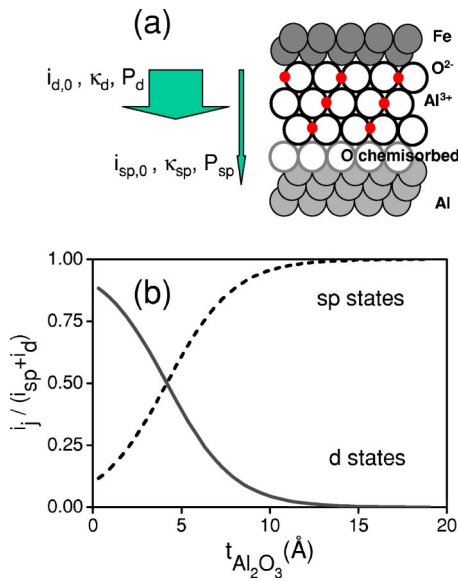


FIG. 1. (a) Parameters determining the sp - and d -like currents through the Al_2O_3 oxide barrier carrying a polarization P_{sp} and P_d . (b) Calculation with Eq. (2) of the text using $i_{sp,0}=0.1$, $\kappa_{sp}^{-1}=0.68 \text{ \AA}$ and $i_{d,0}=0.9$, $\kappa_d^{-1}=0.5 \text{ \AA}$.

1×10^{-6} Torr to 2×10^{-1} Torr O_2 . A significant activation of the oxidation process starts for higher dosages of 1×10^{-5} Torr s. The Al-O bonding relaxes to the bulk value within one monolayer of the oxide,²⁰ implying that starting with the second monolayer the barrier height is comparable to the bulk. The transparency of a one to two monolayer thick barrier has been studied with ballistic electron emission microscopy (BEEM) experiments.²¹ Metallic pinholes and low energy defect channels form single electron conduction channels. They are identified as a reason for a broadened conduction band edge that is observed in the I/V characteristics. Higher exposures (3×10^{-2} Torr s) reduce this conduction channel sufficiently and the barrier is pinhole free.²¹

In superconducting tunneling, the gap region of the superconductor reveals immediately if the barrier is pinhole free: since additional conduction channels open if pinholes are present, besides tunneling, would lead to conduction within the gap region. A detailed discussion of using this criterion to identify pinhole free junctions is well known and was recently discussed by Åkerman *et al.* specifically for the case of MTJs.²² In the following, tunneling will only be discussed for O_2 dosages higher than $p_{\text{O}_2}=8 \times 10^{-2}$ Torr s.

For ultrathin barriers the interface plays a more important role and the model can be very complex^{23,24} for a realistic system. Essentially replacing an array of barriers simulating the rounding of the barrier by a solid one leads to a reduction of the effective barrier height. An analysis using the Simmons or Brinkman formula^{24,25} with a value for the barrier of 2.4 eV fits the I/V spectra on a wide range of the barrier thickness.²⁶ We define a concept of two barrier thicknesses: a *structural thickness*, defined by the real oxide barrier thickness, and a *tunneling thickness* as seen by the tunneling electron. The difference can be attributed by a distribution of barrier thickness on the atomic scale. The regions contribute to the macroscopic tunneling current in parallel. Hence the

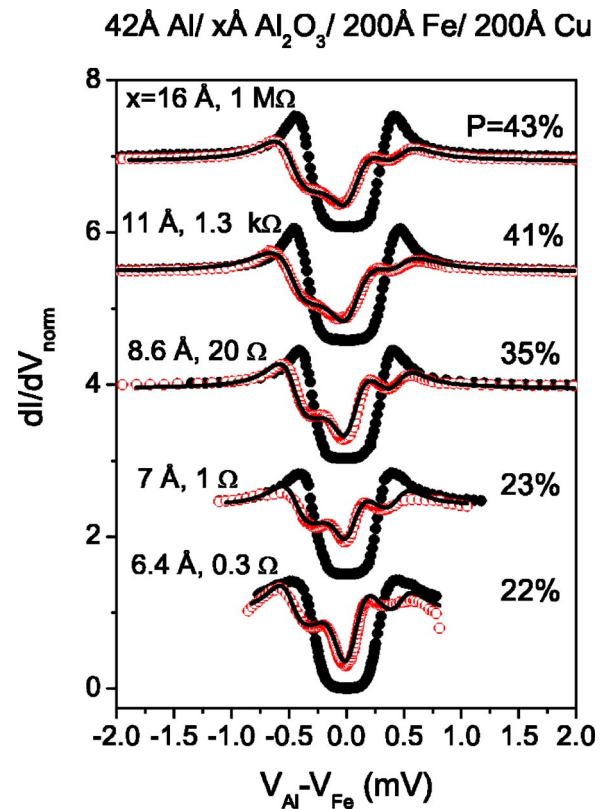


FIG. 2. Tunneling spectra measured with the Meservey-Tedrow method for a $\text{Al}/\text{Al}_2\text{O}_3/\text{Fe}$ junction. The conductance curves have been shifted by a constant amount for clarity. Shown are the data for 0 T (filled symbols) and 3.3 T (open symbols). The fits are given by the solid lines as described in the text.

tunneling thickness will be determined by regions with a thinnest barrier.

For the experiments an Al film is deposited as a superconducting electrode. The Al film is optimized for smoothness (rms roughness < one monolayer). Homogeneity of the film is a prerequisite for the demanding experiment (high superconducting critical field > 4 T). To yield these properties the films are grown in a narrow region of optimized thickness and temperature range (< 100 K). The barrier thickness t was varied by decreasing the thickness of the Al layer and varying the plasma oxidation time ($p_{\text{O}_2}=8 \times 10^{-2}$ Torr) from 1 s to 180 s and natural oxidation time from 20 s to 100 s ($p_{\text{O}_2}=7.5 \times 10^{-2}$ Torr) leaving a ~ 3.8 nm thick film of Al. In this way the only thing to change is the barrier thickness. Shadowing and edge effects are excluded by using a definition mask which can yield a junction of area $80 \times 80 \mu\text{m}^2$ in the middle.

Tunnel conductance measured at 0.45 K as a function of bias voltage is displayed in Fig. 2 for different barrier thicknesses from 6.4 Å to 16 Å. In zero field, the conductance curves show the energy gap of the superconducting density of states in Al. These quasiparticle excitation peaks are broadened by the finite temperature. For the thinner barrier junctions (with correspondingly high conductance) a small additional broadening by current driven effects or heating is observed. An effect on the polarization by a small asymmet-

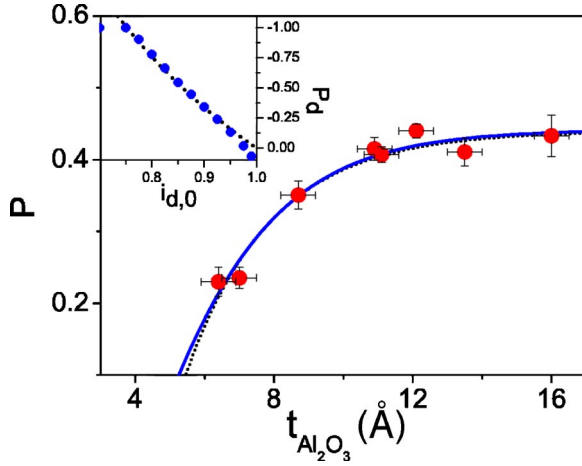


FIG. 3. Spin polarization extracted from the conductance spectra by using Maki's theory for several field values (2.3, 2.6, and 3.3 T and also zero field). The analytical function (continuous line) was calculated by Eq. (4) assuming two spin currents (ps - and d -electron-like). Dotted line is an approximation using Eq. (8). The inset shows the dependence of the polarization P_d on the value assumed for the interface current $i_{d,0}$. The points are fitting values for P_d keeping $i_{d,0}$ fixed. The dotted line is calculated by Eq. (9).

ric reduction of the conduction peak values has been estimated to be not significant and within the error bars. Insignificant conductance at zero bias in the absence of an applied field shows the high quality of the junctions. In the presence of an applied field of 3.3 T parallel to the film plane the quasiparticle density of states is split into spin up and spin down peaks separated by the Zeeman energy. The asymmetry of the conductance peaks is due to spin polarized tunnel current from the ferromagnet. The exact values of the spin polarization are analyzed with a model based on a theory by Maki.²⁷ For high resistance junctions the conductance peaks reveal the well-known polarization of Fe: around 44% for thicker Al_2O_3 barriers.¹ A significant change appears for a junction resistance below about 10Ω (corresponding to a tunneling thickness of about 8 Å): for the thinner barriers the spin down channel starts to increase and the spin polarization drops by a factor of 2 to a value of 22%. Figure 3 shows a plot of the polarization values as a function of the barrier thickness as seen in a tunneling experiment—the polarization starts to decrease below 10 Å Al_2O_3 barrier thickness.

In order to understand the drop in polarization we assume that the tunneling current is carried by i_{sp} and i_d currents having different decay lengths κ_{sp} and κ_d as given by Eq. (2). The total polarization P of the spin current now arises from two currents having polarization P_d and P_{sp} ,¹⁹

$$P(i_{sp} + i_d) = P_{sp}i_{sp} + P_d i_d. \quad (3)$$

Combining Eq. (3) with Eqs. (1) and (2) one can write the effective polarization as

$$P = \frac{P_{sp}i_{sp,0}e^{-\kappa_{sp}t} + P_d i_{d,0}e^{-\kappa_d t}}{i_{sp,0}e^{-\kappa_{sp}t} + i_{d,0}e^{-\kappa_d t}}. \quad (4)$$

The thickness dependence of the polarization is thus described by six parameters. The interfacial currents $i_{sp,0}$ and

$i_{d,0}$ normalized to the total current are related by

$$i_{sp,0} + i_{d,0} = 1. \quad (5)$$

The polarization for the sp -like contribution is well known for the limit of thick barriers $P_{sp}=44\%$ and reduces the free parameter to 4.

Keeping $i_{sp,0}$ fixed, two different limiting cases can be considered: (i) For a smaller contribution of d -like currents $i_{d,0}=0.75$, analyzing with Eq. (4) yields a polarization of $P_d=-1$. A high negative spin polarization is needed to simulate the decrease in spin polarization. Keeping κ_{sp}^{-1} fixed at 0.35 Å the decay length for the d -like current inside the barrier is $\kappa_d^{-1}=0.30$ Å. (ii) For a high contribution of d -like currents of $i_{d,0}=0.98$ the polarization value is $P_d=-0.027$. Only a low negative polarization value is needed to get the same drop in polarization due to the high contribution of the d -like states to the total current. Keeping κ_{sp}^{-1} fixed at 0.35 Å again, we get a decay length for the d -like current of $\kappa_d^{-1}=0.29$ Å. The decay lengths are comparable to theoretical calculations known for other barrier materials.⁶

This reveals that polarization and spin injected currents at the interface are *not* completely independent for the thickness range $t > 6$ Å within the model: a highly negative polarized d -like spin polarization leads to a similar drop of polarization as a high contribution of d -like current with quenched polarization. The inset in Fig. 3 shows the systematic dependence: the fitted polarization value P_d is plotted versus $i_{d,0}$. For values of $i_{d,0}$ between 0.75 to 0.99 the dependence $P_d(i_{d,0})$ shows almost a linear drop of the polarization with increasing $i_{d,0}$. In the following we show that this dependence can also be seen analytically by defining a parameter a

$$a = P_d \frac{i_{d,0}}{i_{sp,0}}, \quad (6)$$

and the difference in the inverse decay length

$$\phi = \kappa_{sp} - \kappa_d. \quad (7)$$

Using these new quantities, Eq. (4) can be rewritten as

$$P = \frac{P_{sp} + a e^{-\phi t}}{1 + \frac{i_{d,0}}{i_{sp,0}} e^{-\phi t}} \approx P_{sp} + a e^{-\phi t}. \quad (8)$$

The latter approximation can be made if the factor $i_{d,0}/i_{sp,0}e^{-\phi t} \ll 1$, which is a rather good approximation for not too small contributions of the sp -like current. The simplified approach yields $a=-3.04(40)$, $P_{sp}=0.44(1)$, and $\phi=0.4(1)$ Å⁻¹ and describes the data within the thickness range from 6 to 16 Å (Fig. 3). Using Eqs. (5) and (6) we get an analytical function for $P_d(i_{d,0})$, Eq. (9), that is plotted in the inset of Fig. 3,

$$P_d = -3.04 \frac{(1 - i_{d,0})}{i_{d,0}}. \quad (9)$$

Taking values of the interfacial currents for Fe using the conductance evaluated from the surface density of states from (Ref. 8), the interfacial current arising from d -like

states is three times the value of sp -like states. In this case, we calculate for $P_d = -100\%$ spin polarization of the d -like states, a very high negative polarization as it is expected from the two current model.⁵ This high polarization value for the d states is not usable for a device with an Fe electrode and Al_2O_3 barrier: extrapolated to the direct interface the spin current arising from sp - and d -like states together will be only -64% and decreases very rapidly towards $P=0\%$. Other types of barriers with different interface bonding promoting only the highly polarized d states may be a way out.¹⁶

One can attribute a low value of the spin polarization of the spin current in ultrathin barriers to alternative mechanisms than d -like contributions to the tunneling current, e.g., small metallic pinholes or a spin flip during the tunneling process. The first mechanism is unrealistic when one observes essentially no leakage current in the conductance spectra at 0.45 K as mentioned before. Channeling with spin-flip through low energy defects in the barrier or spin relaxation within states inside the barrier^{28,29} would quench the polarization but not change the sign and always be present even in thicker barriers and thus can be excluded by our analysis. In addition these defect states are mostly local-

ized in the tail of the density of states and not at small voltages.²⁴

In summary, we have directly observed for the first time a reduction of the polarization of the tunneling current by a factor of 2 for ultrathin barriers using the Meservey-Tedrow technique. It can be described by applying a two current model with the two contributions of the spin current from itinerant sp - and localized d -like electrons within an extension of a model proposed by Stearns already in the seventies. This fundamental study gives a new insight in the tunneling process and shows new ways to find devices with high spin currents by engineering the interface bonding. In addition to the fundamental question addressed, we reveal that tailoring TMR elements using thinner Al_2O_3 barriers in order to keep the resistance low will inherently coincide with a low spin polarization.

We thank Dr. T. H. Kim for providing Maki's theory program to fit the data as well as valuable discussions. We are grateful to Dr. R. Meservey for his keen interest and fruitful discussions. Funding for this work is provided by NSF and ONR grants.

*Author to whom correspondence should be addressed. Electronic address: mmuenze@gwdg.de; present address: IV. Phys. Institut, Universität Göttingen, 37077 Göttingen, Germany.

¹R. Meservey and P. M. Tedrow, Phys. Rep. **238**, 173 (1994).

²J. S. Moodera and G. Mathon, J. Magn. Magn. Mater. **200**, 248 (1999).

³D. J. Monsma and S. S. P. Parkin, Appl. Phys. Lett. **77**, 720 (2000).

⁴R. J. Soulen, Jr., J. M. Byers, M. S. Osofsky, B. Nadgorny, T. Ambrose, S. F. Cheng, P. R. Broussard, C. T. Tanaka, J. Nowak, J. S. Moodera, A. Barry, and J. M. D. Coey, Science **282**, 85 (1998).

⁵M. B. Stearns, J. Magn. Magn. Mater. **5**, 167 (1977).

⁶W. H. Butler, X. G. Zhang, T. C. Schulthess, and J. M. MacLaren, Phys. Rev. B **63**, 054416 (2001).

⁷P. Mavropoulos, N. Papanikolaou, and P. H. Dederichs, Phys. Rev. Lett. **85**, 1088 (2000).

⁸E. Yu. Tsymbal and D. G. Pettifor, J. Phys.: Condens. Matter **9**, L411 (1997); I. I. Oleinik, E. Yu. Tsymbal, and D. G. Pettifor, Phys. Rev. B **62**, 3952 (2000).

⁹J. Mathon and A. Umerski, Phys. Rev. B **63**, 220403(R) (2001).

¹⁰S. Zhang, P. M. Levy, A. C. Marley, and S. S. P. Parkin, Phys. Rev. Lett. **79**, 3744 (1997).

¹¹J. C. Slonczewski, Phys. Rev. B **39**, 6995 (1989).

¹²I. I. Mazin, Phys. Rev. Lett. **83**, 1427 (1999).

¹³J. S. Moodera, M. E. Taylor, and R. Meservey, Phys. Rev. B **40**, 11 980 (1989).

¹⁴J. J. Sun and P. P. Freitas, J. Appl. Phys. **85**, 5264 (1999).

¹⁵P. LeClair, H. J. M. Swagten, J. T. Kohlhepp, R. J. M. van de Veerdonk, and W. J. M. de Jonge, Phys. Rev. Lett. **84**, 2933 (2000).

¹⁶J. M. De Teresa, A. Barthélémy, A. Fert, J. P. Contour, F. Montaigne, and P. Seneor, Science **286**, 507 (1999).

¹⁷M. Sharma, S. X. Wang, and J. H. Nickel, Phys. Rev. Lett. **82**, 616 (1999).

¹⁸W. Wulfhekel, M. Klaua, D. Ullmann, F. Zavaliche, J. Kirschner, R. Urban, T. Monchesky, and B. Heinrich, Appl. Phys. Lett. **78**, 509 (2001).

¹⁹S. F. Alvarado and Ph. Renaud, Phys. Rev. Lett. **68**, 1387 (1992); S. F. Alvarado, *ibid.* **75**, 513 (1995).

²⁰J. Stöhr, L. I. Johansson, S. Brennan, M. Hecht, and J. N. Miller, Phys. Rev. B **22**, 4052 (1980).

²¹W. H. Rippard, A. C. Perrella, F. J. Albert, and R. A. Buhrman, Phys. Rev. Lett. **88**, 046805 (2002); A. C. Perrella, W. H. Rippard, P. G. Mather, M. J. Plisch, and R. A. Buhrman, Phys. Rev. B **65**, 201403 (2002).

²²J. J. Åkerman, J. M. Slaughter, R. W. Dave, and I. K. Schuller, Appl. Phys. Lett. **79**, 3104 (2001).

²³P. Rottländer, M. Hehn, and A. Schuhl, Phys. Rev. B **65**, 054422 (2002).

²⁴J. G. Simmons, J. Appl. Phys. **34**, 1793 (1963); J. Phys. D **4**, 613 (1971).

²⁵W. F. Brinkman, R. C. Dynes, and J. M. Rowell, J. Appl. Phys. **41**, 1915 (1970).

²⁶Taking 1 eV instead of 2.4 eV would increase the barrier thickness by 1.9 Å (at a barrier thickness of 4.5 Å) and by 1 Å (at 8 Å). This is within the error bars given in Fig. 3.

²⁷K. Maki, Prog. Theor. Phys. **32**, 29 (1964); D. C. Worledge and T. H. Geballe, Phys. Rev. B **62**, 447 (2000).

²⁸W. Rudzinski and J. Barnas, Phys. Rev. B **64**, 085318 (2001).

²⁹D. Bagrets, A. Bagrets, A. Vedyayev, and B. Dieny, Phys. Rev. B **65**, 064430 (2002).